Eur. Phys. J. B **15**, 435–443 (2000)

THE EUROPEAN PHYSICAL JOURNAL B

EDP Sciences

The scattering and transmission of elastic waves in quasi-two-dimensional planar waveguides with linear defect boundaries

M. Belhadi[1], O. Rafil[1], R. Tigrine[1], A. Khater[2,a], J. Hardy[3], A. Virlouvet[2], and K. Maschke[4]

[1] Département de Physique, Institut des Sciences Exactes, Université Mouloud Mammeri de Tizi-Ouzou, 15000 Tizi-Ouzou, Algeria
[2] Laboratoire de Physique de l'État Condensé[b], Université du Maine, 72085 Le Mans, France
[3] Laboratoire d'Acoustique[c], Université du Maine, 72085 Le Mans, France
[4] Institut de Physique Appliquée, École Polytechnique Fédérale, 1015 Lausanne, Switzerland

Received 8 November 1999 and Received in final form 14 January 2000

Abstract. The influence of linear defect boundaries on the transmission and scattering of elastic waves in quasi-two-dimensional wave-guides is studied using the matching method. A linear defect boundary separating two wave-guide crystalline lattice domains is characterised here by a linear chain of defect masses and by modified elastic constants in the boundary, different from their values in the bulk of the domains. In particular a square lattice is considered to model the domains of the two-dimensional planar wave-guide containing the linear defect. The reflection and transmission probabilities, and the total transmission probabilities are calculated numerically and presented for the scattering processes in a variety of cases. We show that the interaction between the localised modes introduced by the defect boundary and the propagating modes of the system leads to Fano resonances. These resonances shift to higher (lower) frequencies for smaller (larger) defect masses, and for the same mass as function of the angle of the incident wave. Other spectral features shown to exist are due to interference effects especially at oblique incidence and when modifying the boundary elastic constants.

PACS. 61.46.+w Clusters, nanoparticles, and nanocrystalline materials – 61.12.Bt Theories of diffraction and scattering – 68.65.+g Low-dimensional structures (superlattices, quantum well structures, multilayers): structure, and nonelectronic properties

1 Introduction

The electronic transport and quantum interference in low dimensional mesoscopic systems with defects have been intensively studied [1–6]. The recent research, oriented towards the study of electronic scattering in quasi-one-dimensional systems, has been motivated by the need to understand the limitations that structural disorder, or other kinds of disorder, may have on the physical properties of microelectronic devices.

The study of scattering of elastic waves in low dimensional mesoscopic systems, in contrast, is of more recent theoretical interest for systems which may yield useful information [7,8]. The properties of waves in the neighbourhood of isolated inhomogeneities differ from those in ideal systems and are more complicated. The inhomogeneities modify the vibrational properties of the system giving rise to new localised modes in their neighbourhood, they can also scatter incident phonons. The scattering and transmission of elastic waves in low dimensional systems with defects is of interest owing to high technology advances that permit the construction of low dimensional nanometric devices for which these effects become pronounced. The motivation of the present paper lies in the study of the increasingly important elastic properties of nanostructures in surfaces.

The analysis presented is for the scattering of vibrational waves by linear defect boundaries in crystalline quasi-two-dimensional planar wave-guides. The wave-guide is described as a square lattice with one mass per unit cell. The linear defect is treated as a perturbed boundary between two semi-infinite planes as shown in Figure 1, each plane containing identical masses. The defect is consequently a linear chain of defect masses which constitute the boundary between the two semi-infinite lattice planes. Such a defect boundary is also characterised by local elastic constants that may differ from their homogeneous values in the bulk of the planar wave-guides.

Quasi-two-dimensional crystals do indeed exist and include systems of differing nature [10]. An early

[a] e-mail: khatter@aviion.univ-lemans.fr
[b] UPRES-A 6087
[c] UMR 6613

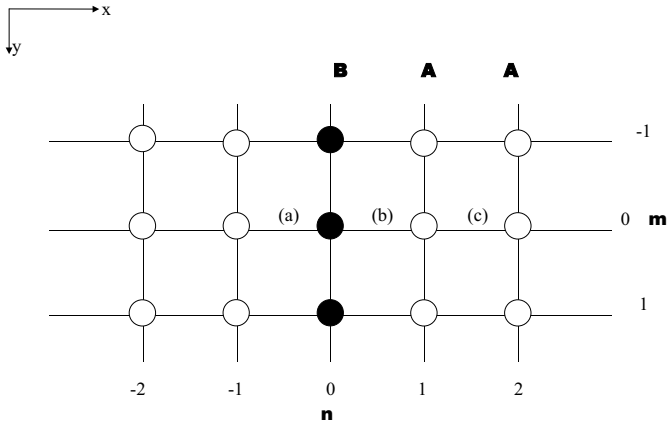

Fig. 1. A schematic representation of a linear defect boundary, modelled as an infinite linear chain of impurity objects B with mass $m_{\rm d}$ between two semi-infinite square lattices of identical objects A of mass m. The elastic constants in the boundary may also be different from the rest of the system.

example concerns the atomic solid He layer adsorbed on solid surfaces, that plays a fundamental role in the heat conductance across a solid-liquid He interface [9]. Other well known examples are 2D lattices formed by atoms adsorbed on the surface of crystal substrates. The physisorbed noble gas films on close-packed atomic planes of metal surfaces and on graphite, [11,12], serve as representative systems for studying 2D crystalline structures. The periodic potential corrugation of the substrate surface engenders an extensive variety of 2D structures in the adsorbed system, usually divided into commensurate and incommensurate classes [13]. The incommensurate phase may split up into commensurate lattice domains, separated by linear defects called domain walls or solitons. These are effectively grain boundaries. Heavy and superheavy solitons correspond to the presence of extra mass on the grain boundaries [10,14].

Two-dimensional phonons may be excited, thermally or by other experimental techniques, such as high resolution Helium Atom Scattering HAS, [15], in the quasi-2D lattice. These phonons may undergo transmission and reflection at the linear defect domain boundaries. The *inelastic* scattering of 2D phonons in the 2D solid He atomic layers owing to surface defects, has been shown to be part of the mechanism that explains the anomalous Kapitza thermal conductance normal to the solid-liquid He interface [9].

In the present work we look, in contrast, for the *elastic* scattering of this type of 2D phonon by linear defects in the plane of the surface. In particular the model presented has as a primary objective, the analysis and characterisation of the influence of these defects on the scattering of these waves in a quasi-two-dimensional system, as in the above 2D crystalline adsorbates. The model may equally serve for the study of these scattering effects in macroscopically constructed systems.

To the authors knowledge there are no experimental results at present to compare with. The difficulty with this kind of experiment is to be able to have a sufficiently local spectroscopic probe to distinguish the incident from the transmitted elastic spectra across the linear defect. The high resolution Helium Atom Scattering HRHAS [15], though not sufficiently local at the present time, may be eventually a realistic approach. However, the model applies equally on the macroscopic scale, and it is possible to test the theoretical results *via* an experiment using laboratory scale masses, binding springs, and wave generators as in acoustical studies.

A description of the model is given in Section 2. The dynamical properties of the perfect semi-infinite crystalline 2D planar wave-guide are presented in Section 3, followed by a brief outline of the formalism for scattering at the defect in Section 4. The results and discussion are presented in Section 5.

2 Model

Our structural model in Figure 1 is constructed from two semi-infinite square lattices of identical objects A, each of mass m, separated by a boundary that is an extended linear chain of identical impurity objects B, each of mass $m_{\rm d}$. The quantity $e = m_{\rm d}/m$ denotes their ratio. Nearest neighbour (nn) elastic constants K_1 and next nearest neighbour (nnn) elastic constants K_2, are taken to represent the possible A–A, B–B and A–B interactions in the harmonic approximation [16]. Next nearest neighbours elastic interactions exist, they ensure the stability of crystalline structures, and permit the propagation of measurable transverse modes in these systems. In fact these interactions are an approximation for more elaborate many body potentials that bind the atoms elastically even beyond nnn interactions [17].

The elastic interactions in the bulk of the 2D semi-infinite A lattices are considered to be the same. Let $r = K_2({\rm A}{-}{\rm A})/K_1({\rm A}{-}{\rm A})$ be their ratio. In the neighbourhood of the linear defect boundary these interactions may be modified. They shall be denoted by the complete set $r_{\rm d1} = K_1({\rm B}{-}{\rm B})/K_1({\rm A}{-}{\rm A})$, $r_{\rm d3} = K_1({\rm A}{-}{\rm B})/K_1({\rm A}{-}{\rm A})$, and $r_{\rm d4} = K_2({\rm A}{-}{\rm B})/K_1({\rm A}{-}{\rm A})$. Note that there are no nnn K2(B–B) elastic interactions. Let the constant a measure everywhere on the square lattice, the distance between nearest neighbour objects along the Cartesian x and y directions.

3 Dynamical properties

A number of methods exist to study the vibrational dynamics of such crystalline systems. The matching method that we employ in this paper, has previously been extended to study wave scattering at defects and nanostructures in quasi-one-dimensional crystalline systems, [7,8]. This method allows one to deal with both aspects of localised modes and of wave scattering, within the same mathematical framework.

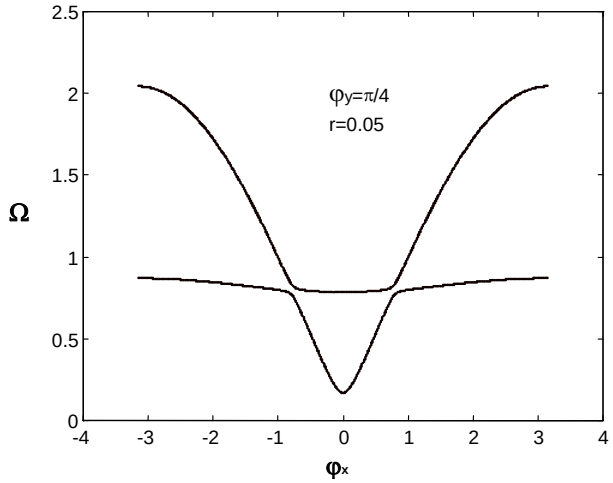

Fig. 2. Typical phonon dispersion curves for the A lattice planar wave guide presented over the $\varphi_x = [-\pi, \pi]$ 1st BZ, for the case of $\varphi_y = \pi/4$, using $r = 0.05$.

The equation of motion of a mass at site l is given as usual in the harmonic approximation by

$$\omega^2 m(l) U_\alpha(l,\omega) = -\sum_{l' \neq l} \sum_{\beta} K(l,l') \frac{r_\alpha r_\beta}{d^2} \times [U_\beta(l,\omega) - U_\beta(l',\omega)] \quad (1)$$

for α, $\beta \in \{x, y\}$. Consider that $m(l) \equiv m$ for all sites l in the semi-infinite A lattice planar wave-guides, $U_\alpha(l,\omega)$ is the displacement field along the α Cartesian direction, r_α is the α component of the radius vector and d the distance, between the sites l and l'.

The dispersion curves of the elastic waves away from the linear defect boundary, that is to say in the bulk of the semi-infinite A lattices, may be described by the travelling wave solutions of the equation of motion, equation (1), in the perfect planar wave-guide.

The motion on a site (n, m) outside the linear defect boundary, may hence be expressed as

$$[\Omega^2 I - D(z, \varphi_y)]|U\rangle = 0 \quad (2)$$

where Ω is a dimensionless frequency determined from $\Omega^2 = \omega^2/\omega_0^2$. The frequency ω_0, characteristic of the system, is given by $\omega_0^2 = K(l,l')/m$, for l and l' nearest neighbours, and $D(z, \varphi_y)$ is the dynamical matrix.

The frequency squared Ω^2 and the $U_{l,m}(\Omega, q)$ components are the eigenvalues and eigenvectors of the dynamical matrix in the bulk of the square semi-infinite A lattice. The bulk dispersion curves are obtained by setting $z = \exp(\mathrm{i}\varphi_x)$ and inserting this in equation (2) where the quantities $\varphi_x = q_x a$ and $\varphi_y = q_y a$ are dimensionless and span the 2D Brillouin Zone, (q_x, q_y) is the reciprocal lattice wavevector. Typical results, for $r = K_2(\mathrm{A}{-}\mathrm{A})/K_1(\mathrm{A}{-}\mathrm{A}) = 0.05$, are presented in Figure 2 for the dispersion curves in the BZ of φ_x at a wavevector component of $\varphi_y = \pi/4$. Note that the normalised components (φ_x, φ_y) give the angle of incidence of the incoming wave.

In order to describe the scattering problem in the presence of linear defect boundaries, we have not only to know the propagating modes described above *via* their dispersion curves, but also to consider the evanescent solutions of the system. In other words, for a given Ω, we need all the solutions $z(i)$, including those with $|z(i)| \neq 1$.

The evanescent and the propagating fields in the semi-infinite A lattices, away from the linear defect boundary, are described in general by the phase factor doublets $\{z(i), z(i)^{-1}\}$, as one goes from one site to its nearest neighbours along the direction normal to the symmetry direction of the linear defect. The evanescent and propagating fields, determined respectively by the conditions $|z(i)| < 1$, and $|z(i)| = 1$, are given, [7,8], as the solutions of the equation of the motion in the bulk of these planar lattices.

A non trivial solution for the dynamical matrix requires that the determinant of $[\Omega^2 I - D(z, \varphi_y)]$ vanish. This then gives a characteristic secular equation in z, that may be expressed in the polynomial form for the A lattice planar wave-guide

$$A_0 + A_1 z + A_2 z^2 + A_1 z^3 + A_0 z^4 = 0 \quad (3)$$

where A_n are coefficients that depend on Ω, φ_y, and the elastic constants of the planar wave-guide. One can show that the phase factor doublets $\{z(i), z(i)^{-1}\}$ both verify the polynomial, owing to the hermitian nature of bulk dynamics or time reversal symmetry in crystalline lattices [18].

For non propagating modes on the A square lattice planar wave-guide, only two physically acceptable evanescent solutions for z are retained from the roots of equation (3). Since for propagating modes each of the phase factors contains the same information, we consider only two modes propagating from the left to the right. These solutions are called eigenmodes 1 and 2.

The functional behaviour of these modes may be graphically illustrated by the loci $\Omega(z)$ on and inside a unit circle in the complex plane. Typical loci are presented in Figure 3, in three-dimensional phase space, for the case characterised by $\varphi_y = \pi/4$, and for different values of the ratio r, ranging from 0.05 to 0.5 by increments of 0.05. Note that the lowest locus in these figures, given for $r = 0.05$, corresponds effectively to the dispersion curves in Figure 2. The evanescent modes are represented by curves inside the unit circle in the complex plane.

4 Scattering at the defect boundary

To treat the scattering problem fully, a knowledge of both the propagating and the evanescent modes is needed to describe the scattering solutions in the presence of the linear defect boundary. The evanescent modes do not transport energy but they are necessary for a full description of the scattering problem. Since the perfect square A lattice planar wave-guide does not couple between different eigenmodes, the scattering problem for each eigenmode may be treated separately.

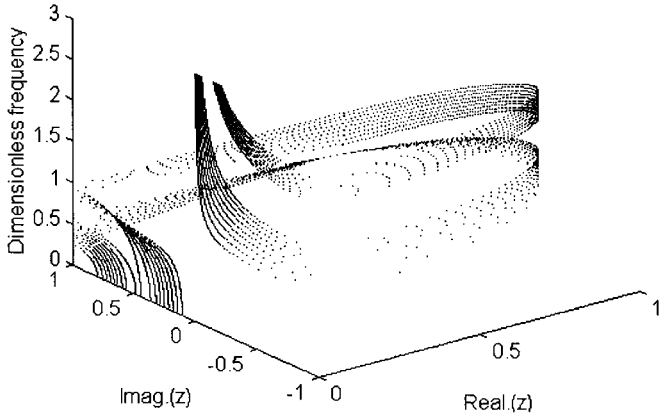

Fig. 3. A typical three-dimensional view of the vibrational eigenmodes $\Omega(z)$ for the two-dimensional A lattice planar waveguide, for different values of the ratio r ranging from $r = 0.05$ to $r = 0.5$ through increments of 0.05, for the case the specific case of $\varphi_y = \pi/4$. See the text for details.

For an incoming propagating wave in eigenmode i, incident from the left to right, the scattered waves are reflected back and the transmitted waves forward. The Cartesian displacement field components $U_\alpha(n,m)$ for a mass that lies outside the linear defect boundary, may be expressed using the matching approach [18]. For a site in the region to the left of the linear defect boundary, this can be written as

$$U'_\alpha(n,m) = V_i(z_i)^n + \sum_{i'}(z_{i'})^{-n} R_{i'i} V_{i'}, \quad n < 0 \qquad (4)$$

whereas for a site in the region to the right of the linear defect boundary, this is given as

$$U_\alpha(n,m) = \sum_j (z_j)^n T_{ji} V_j, \quad n > 0. \qquad (5)$$

For an incident wave i, the quantities $R_{i'i}$ denote the reflection coefficients into eigenmodes $i' = 1, 2$, and the quantities T_{ji} are the corresponding transmission coefficients for the $j = 1,\ 2$ eigenmodes. The coefficients V_i , $V_{i'}$, and V_j are the eigenvectors of the dynamical matrix associated to the perfect square A lattice planar wave-guide at the scattering frequency and at the given incident angle.

Let $[|R\rangle, |T\rangle]$ be the basis vector for the reflection and transmission coefficients in a Hilbert space, and $|U\rangle$ be the vector that is composed of the displacements of a set of irreducible sites in the linear defect boundary. The equations of motion for the linear defect coupled to the rest of the planar wave-guides, may be rewritten in terms of the vector $[|U\rangle, |R\rangle, |T\rangle]$. The necessary and sufficient minimum set of sites defining the vector $|U\rangle$, is indicated by the letters (a), (b), (c) in Figure 1. Using the transformations connecting the displacement fields, and substituting these in equations (2), (4) and (5), we obtain a linear inhomogeneous system of equations in the form

$$[\Omega^2 I - D(z,\varphi_y)][|U\rangle, |R\rangle, |T\rangle] = -|IH\rangle \qquad (6)$$

where the vector $-|IH\rangle$, regroups the inhomogeneous terms describing the incident wave, when mapped appropriately onto the basis vectors.

The solution of equation (6) yields the vector $|U\rangle$ for the displacements of the irreducible set of sites in the linear defect boundary, also the reflection and transmission coefficient $R_{i'i}$ and T_{ji} at the scattering frequency and the given incident angle.

In scattering phenomena the reflection and transmission behaviour is described usually in terms of the scattering matrix, which elements are given by the reflection amplitudes $r_{i'i}$ for the backward scattered waves i', and the transmission amplitudes t_{ji} for the forward scattered waves j, per incident propagating mode i. These quantities are given as the square of the respective elements of the scattering matrix. Explicitly, the reflection amplitudes are given by the relation

$$r_{i'i} = (v_{gi'}/v_{gi})|R_{i'i}|^2 \qquad (7)$$

and the transmission probabilities by the relation

$$t_{ji} = (v_{gj}/v_{gi})|T_{ji}|^2. \qquad (8)$$

To satisfy unitarity requirements, the scattered waves have to be normalised with respect to their group velocity

$$v_{gs} = (-1/2\Omega) U_s^t (\mathrm{d}D/\mathrm{d}q) U_s. \qquad (9)$$

The group velocity v_{gs} of the s eigenmode is equal to zero for evanescent modes. Though they do not contribute to energy transfer, the evanescent modes are nevertheless necessary for a complete description of the scattering amplitudes of the multi-channel planar wave-guide.

Further, it is possible to define reflection and transmission probabilities at incident angle φ_y for a given propagating eigenmode i by the following expressions

$$r_{i,\varphi_y}(\Omega) = \sum_{i'} r_{i'i,\varphi_y} \qquad (10)$$

$$t_{i,\varphi_y}(\Omega) = \sum_j t_{ji,\varphi_y}. \qquad (11)$$

In order to describe the overall transmission of the linear defect boundary at the scattering frequency and at the given incident angle in the multi-channel planar wave-guide, it is also useful to define a total transmission probability

$$t_{\varphi_y}(\Omega) = \sum_i \sum_j t_{ji,\varphi_y} \qquad (12)$$

where the sum is carried over all propagating modes. The calculated transmission probabilities $t_{i,\varphi_y}(\Omega)$ per eigenmode i, and the total transmission probability $t_{\varphi_y}(\Omega)$ are variables that are useful to calculate, to be able to compare with experimentally measurable quantities.

5 Results and discussion

For our numerical calculations in the A square lattice planar wave-guide, we have chosen $r = 0.05$, considering that

next-nearest neighbour interactions are weaker than nearest neighbour ones.

The simplest linear defect boundary to study numerically corresponds to a chain of defect masses $e \neq 1$, with no elastic constant modifications, hence to $r_{\mathrm{d}1} = r_{\mathrm{d}3} = 1$ and $r_{\mathrm{d}4} = r = 0.05$. Two situations have been considered, namely the case of light ($e = 0.5$) and of heavy ($e = 5$) defect masses in the boundary.

In Figures 4a and 4b we present, for the case of light $e = 0.5$ defect masses, and for normal incidence $\varphi_y = 0$, the numerical results for the reflection and transmission probabilities in the modes 1 and 2 as a function of scattering frequency Ω. The presence of the linear defect boundary leads as expected to a general decrease of the transmission probabilities with increasing frequency. Note the different frequency intervals in Figures 4a and 4b corresponding to the two propagating modes.

In Figure 4c the total transmission probability or conductance $t_{\varphi_y=0}(\Omega)$ of the system is presented for this case, in comparison with $t_{p,\varphi_y=0}$, which is the ideal conductance of the planar wave-guide in the absence of the linear defect boundary. The histogram step of $t_{p,\varphi_y=0}$ in Figure 4c corresponds for normal incidence, to the change in the number of propagating modes in the different frequency intervals.

In Figures 5a and 5b numerical results are presented for the reflection and transmission probabilities for the incident modes 1 and 2, as a function of scattering frequency Ω, for the case of heavy $e = 5$ defect masses and for normal incidence $\varphi_y = 0$. As expected, the influence of the linear defect boundary is smallest when the scattering frequency $\Omega \to 0$, leading to a maximum in the transmission probabilities $t_{i,\varphi_y=0} \to 1$.

As one increases the frequency, on the other hand, the transmission probabilities may be seen to decrease, going to zero near the zone boundaries. This is observable in Figures 4a, 4b and in Figures 5a, 5b, independently of the strength of the defect, although the approach of $t_{i,\varphi_y=0}$ to zero differs with the strength of the defect. This behaviour, as expected for the case of normal incidence $\varphi_y = 0$, is the same as compared to the case of the linear chain [7], where the introduction of a mass defect influences the transmission probabilities in the same manner.

In Figure 5c the total transmission probability or conductance, $t_{\varphi_y=0}(\Omega)$, of the system, is presented for the case of the heavy defect mass $e = 5$ and for normal incidence, in comparison with $t_{p,\varphi_y=0}$, the ideal conductance of the planar wave-guide for this case. The quantity $t_{p,\varphi_y=0}$ in Figure 5c is naturally the same as that in Figure 4c.

Consider next the consequences of the oblique incidence at the linear defect boundary, at an angle $\varphi_y \neq 0$, of the propagating modes, on the transmission and reflection probabilities. For simplicity, we present the results for only mode 1, for respectively the cases of light ($e = 0.5$), and heavy ($e = 5$) defect masses, and for unmodified elastic constants $r_{\mathrm{d}1} = r_{\mathrm{d}3} = 1$, and $r_{\mathrm{d}4} = 0.05$ in the boundary.

The spectra in Figures 6a, 6b, 6c give the transmission and reflection probabilities for mode 1 into mode 1, on

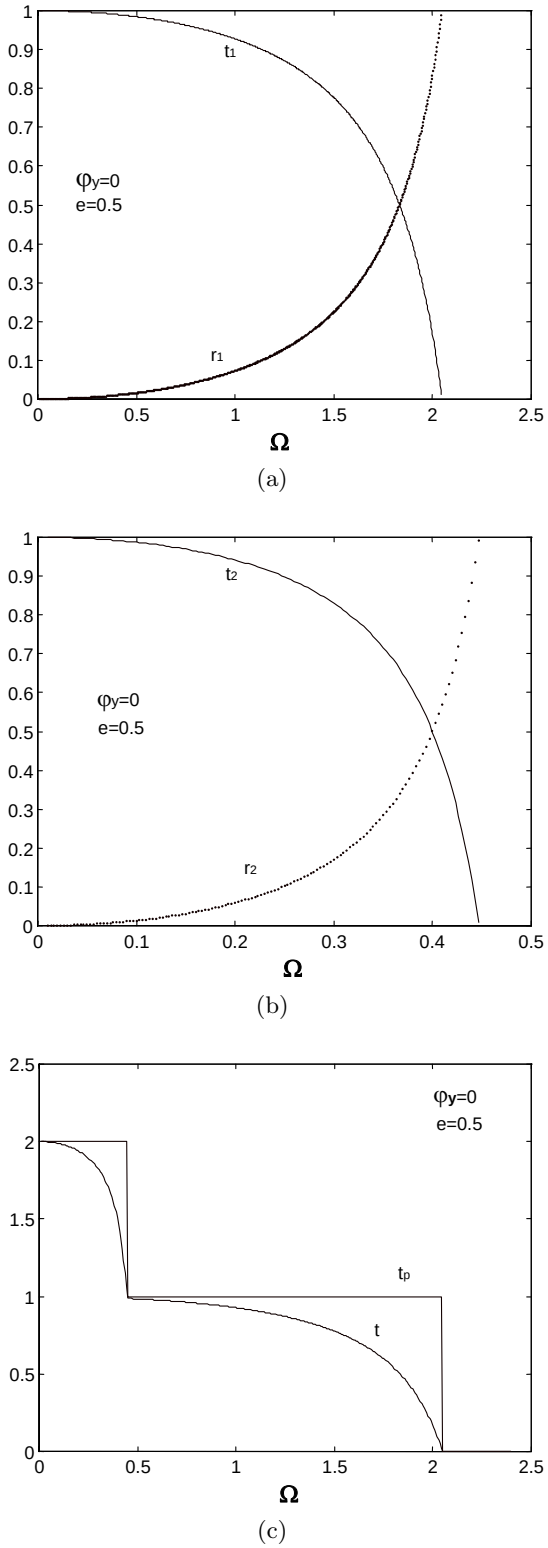

Fig. 4. The transmission and reflection probabilities as a function of the scattering frequency Ω, for the case of light defects, $e = 0.5$, and normal incidence, $\varphi_y = 0$. (a) Mode 1 incident, reflected, transmitted. (b) Mode 2 incident, reflected, transmitted. (c) Total transmission probability or conductance of the system. The elastic constants are not modified in the boundary, and $r = 0.05$ in the A lattice.

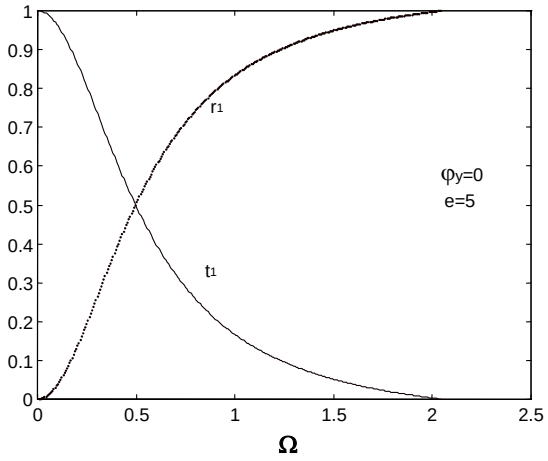

(a)

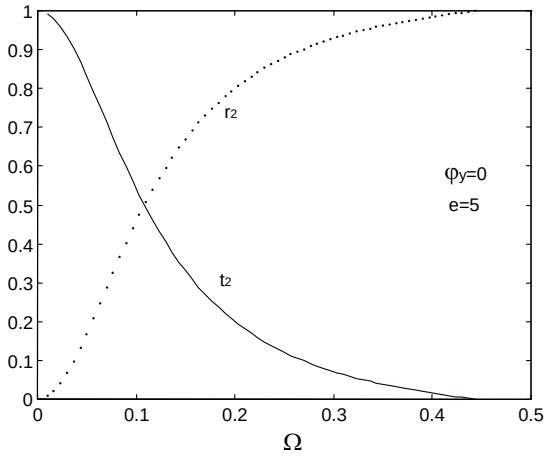

(b)

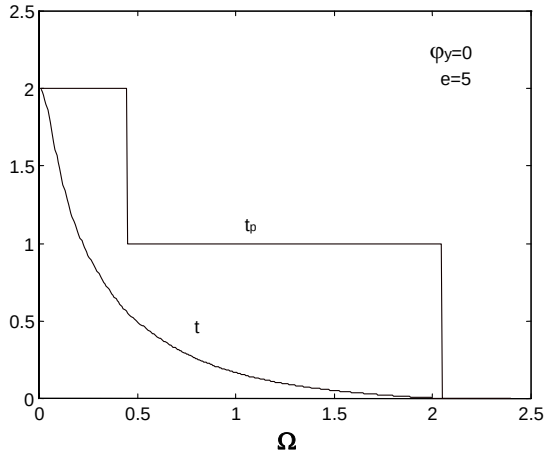

(c)

Fig. 5. The transmission and reflection probabilities as a function of the scattering frequency Ω, for the case of heavy defects, $e = 5$, and normal incidence, $\varphi_y = 0$. (a) Mode 1 incident, reflected, transmitted. (b) Mode 2 incident, reflected, transmitted. (c) Total transmission probability or conductance of the system. The elastic constants are not modified in the boundary, and $r = 0.05$ in the A lattice.

either side of the linear defect boundary, for the case of light defect masses, $e = 0.5$, for respectively $\varphi_y = \pi/6$, $\pi/4, \pi/2$. In contrast the spectra in Figures 7a, 7b, 7c, give the same information but for the case of heavy defect masses, $e = 5$.

Strong resonance features are seen in these processes to superpose on the monotonous decrease of $t_{1,\varphi_y=0}$ observed in Figure 4a, and on the monotonous increase of $r_{1,\varphi_y=0}$ observed in Figure 5a.

The first resonance can be attributed to interference effects of incident and scattered waves due to the change in the polarisation of the vibrational field of the two propagating modes at their cross over. For $\varphi_y = \pi/4$, for example, this cross over is around $\Omega \approx 0.8$. This feature may be seen in succession in Figures 3, 6b, 7b, which illustrate the spectra for this angle of incidence. Note that this first resonance shifts to higher frequencies with increasing incident angle.

The second resonance is due to the presence of defect induced resonant states, interpreted as due to the coupling between the continuum and a discrete state corresponding to a mode of vibration localised in the neighbourhood of the linear defect boundary. In earlier work, [16,18], we have shown that the introduction of a defect, such as an impurity mass, induces localised modes on the defect. This can be hence identified as a Fano like resonance. For $\varphi_y = \pi/4$ this resonance in the spectra is around $\Omega \approx 1.2$.

The presence of these localised states in the linear defect boundary leads to the additional resonances in the calculated spectra in Figures 6a, 6b, 6c and in Figures 7a, 7b, 7c. As may be expected this resonance shifts to higher (lower) frequencies for smaller (larger) defect masses, and as a function of incident angle φ_y values for the same mass.

The effect of a combined linear boundary defect, characterised by defect masses and by simultaneous changes in the boundary elastic constants, on the evolution of the reflection and transmission probabilities is presented in Figures 8a, 8b, 8c and Figures 9a, 9b, 9c, for respectively the cases of light, $e = 0.5$, and heavy $e = 5$, defect masses. The modified boundary elastic constants are the same in both cases and are given by $r_{\rm d1} = 1.1$, $r_{\rm d3} = 1.05$, $r_{\rm d4} = 0.95$, where in the bulk of the wave guides $r = 0.05$ as before.

The combined linear boundary defect shows a stronger resonant structure for the transmission and reflection probabilities, in comparison with the case of a linear defect of impurity masses only. This is due to the interactions of the now more complex features of the localised states in the linear defect boundary, with the propagating modes of the system.

6 Conclusions

In the present paper we have developed an approach that allows us to treat the scattering properties of linear boundary defects in quasi-two-dimensional disordered mesoscopic systems, using a relatively simple model of a square lattice planar wave-guide.

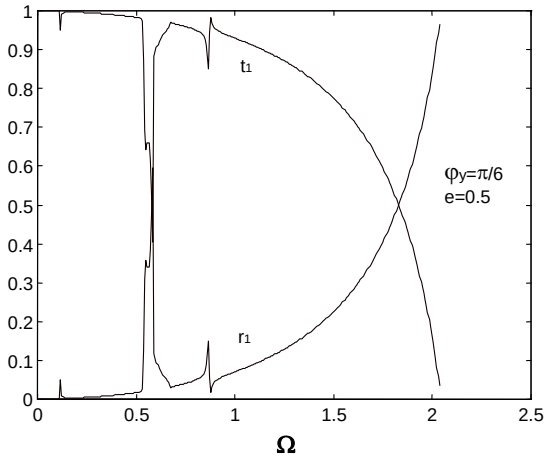

(a)

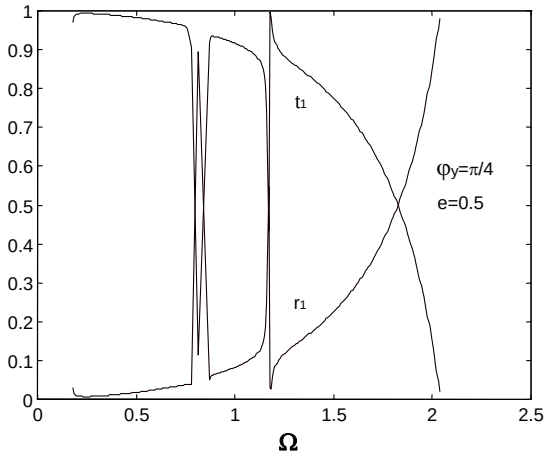

(b)

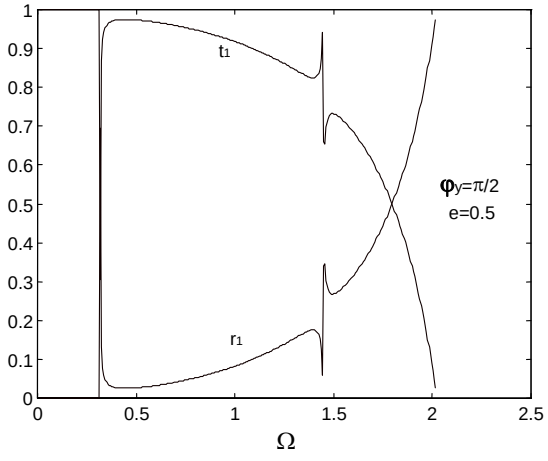

(c)

Fig. 6. The transmission and reflection probabilities for mode 1 as a function of the scattering frequency Ω, for the case of light defects, $e = 0.5$, and for varying angles of incidence: (a) $\varphi_y = \pi/6$, (b) $\varphi_y = \pi/4$, (c) $\varphi_y = \pi/2$. The elastic constants are not modified in the boundary, and $r = 0.05$ in the A lattice.

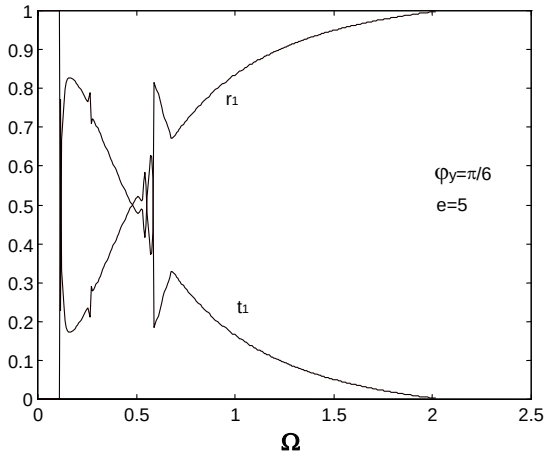

(a)

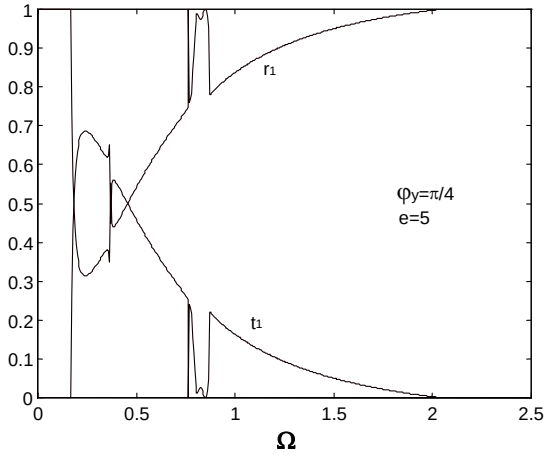

(b)

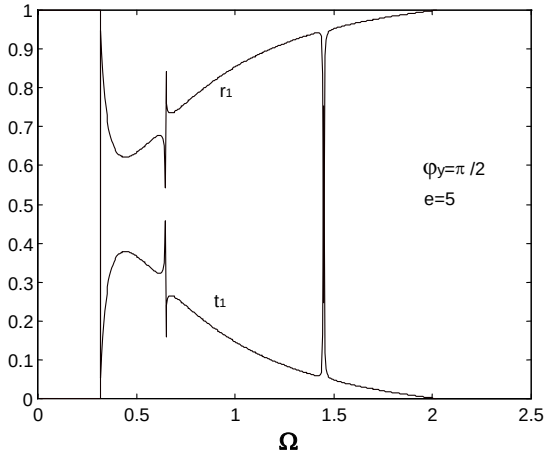

(c)

Fig. 7. The transmission and reflection probabilities for mode 1 as a function of the scattering frequency Ω, for the case of heavy defects, $e = 5$, and for varying angles of incidence. (a) $\varphi_y = \pi/6$, (b) $\varphi_y = \pi/4$, (c) $\varphi_y = \pi/2$. The elastic constants are not modified in the boundary, and $r = 0.05$ in the A lattice.

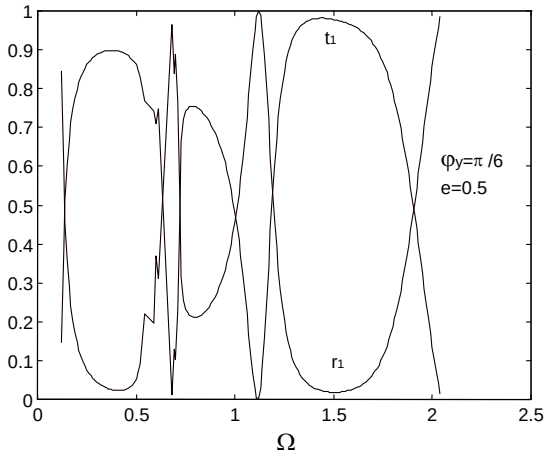

(a)

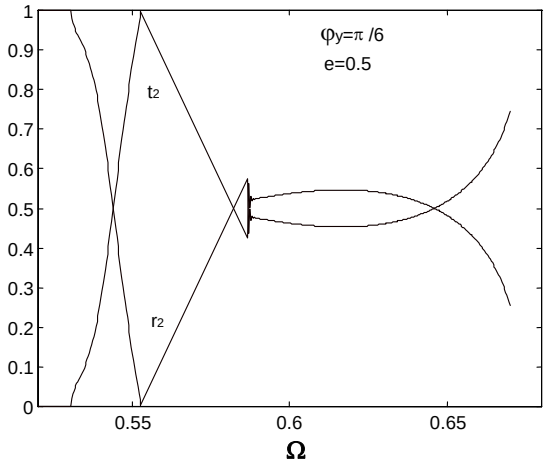

(b)

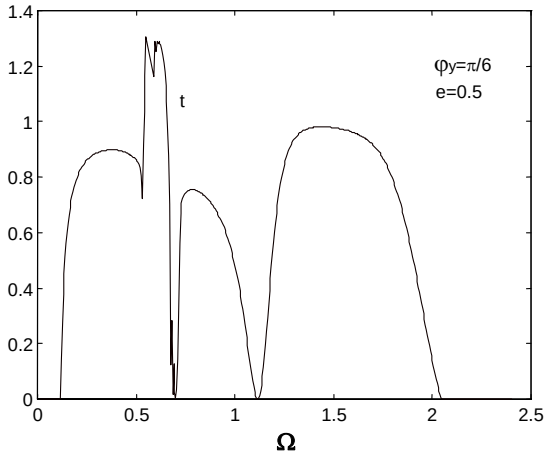

(c)

Fig. 8. The transmission and reflection probabilities for modes 1 and 2, as a function of the scattering frequency Ω, for the case of light defects, $e = 0.5$, $\varphi_y = \pi/6$ incidence, and when the elastic constants are modified in the linear defect boundary: $r_{\mathrm{d}1} = 1.1$, $r_{\mathrm{d}3} = 1.05$, $r_{\mathrm{d}4} = 0.95$. As before $r = 0.05$ in the A lattice. (a) Mode 1. (b) Mode 2. (c) Conductance of the system in this case.

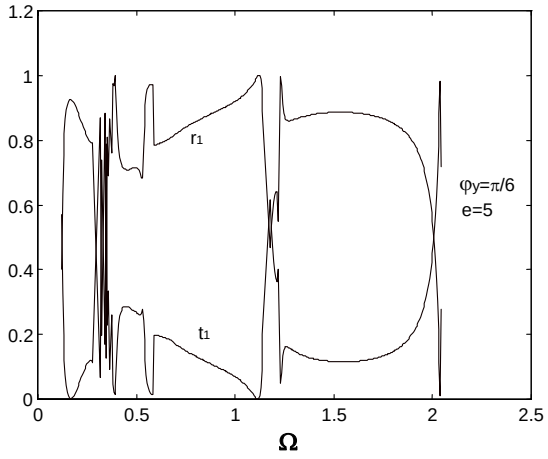

(a)

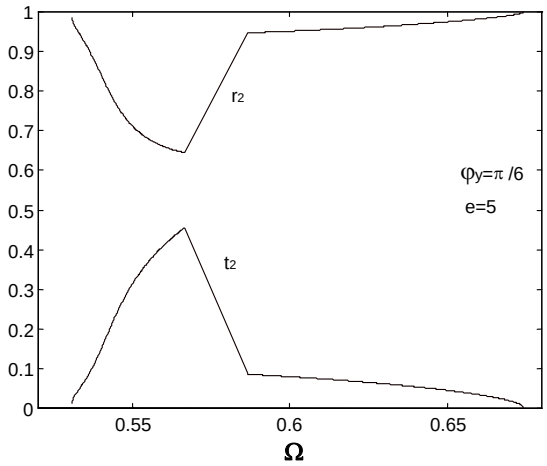

(b)

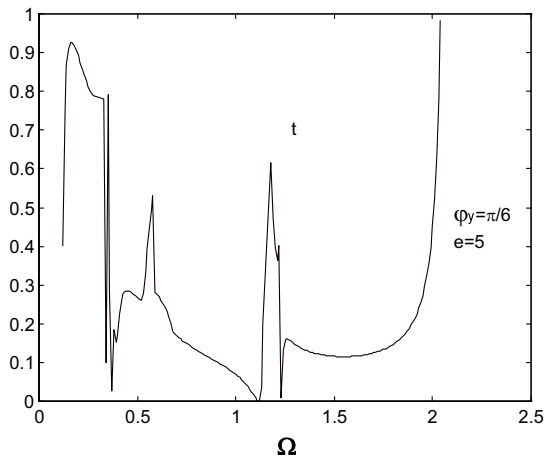

(c)

Fig. 9. The transmission and reflection probabilities for modes 1 and 2, as a function of the scattering frequency Ω, for the case of heavy defects, $e = 5$, $\varphi_y = \pi/6$ incidence, and when the elastic constants are modified in the linear defect boundary: $r_{\mathrm{d}1} = 1.1$, $r_{\mathrm{d}3} = 1.05$, $r_{\mathrm{d}4} = 0.95$. As before $r = 0.05$ in the A lattice. (a) Mode 1. (b) Mode 2. (c) Conductance of the system in this case.

Our numerical results show that in spite of their special character, the scattering of vibrational waves has some features in common with the scattering of electron waves that can be described in terms of basically the same interference phenomena. Other features are not common owing to the vector character of the vibrational field [7]. An example of common features are the Fano resonances, that are usually evoked to describe the interference between propagating transmitted modes and localised modes in the linear defect boundary. It is seen for linear defect boundaries in a quasi two-dimensional crystal that this type of resonance shifts to higher (lower) frequencies for smaller (larger) defect masses, and for the same mass as function of φ_y values.

We have also shown that additional spectral resonances appear which are effectively interference effects due to the interaction between the incident propagating modes with the scattered waves of the system, effects that are induced by the modification of boundary elastic constants and introduction of defect masses. These spectral features are pronounced for the cases of oblique incidence and of elastic constants modified in the linear defect boundary.

The model may be applied to two-dimensional crystals containing domain walls. The best known examples of these systems are 2D lattices formed by atoms adsorbed on the surface of crystal substrates, such as physisorbed noble gas films on close-packed atomic planes of metal surfaces. To the authors knowledge, however, there are no experimental results at present to compare with. The difficulty with this kind of experiment is to be able to have a sufficiently local spectroscopic probe to distinguish the incident from the transmitted elastic spectra across the linear defect boundary. The high resolution Helium Atom Scattering HRHAS, though not sufficiently local at the present time, may be eventually a realistic approach.

On the other hand the model applies equally on the macroscopic scale, and it is hence possible to test the theoretical results *via* an experiment using laboratory scale masses, binding springs, and wave generators, as in acoustical studies.

The formalism presented is an analytical approach independent of the details of the nanostructure of the isolated domain wall, which makes it easy to extend to a variety of real problems. It can also give in a direct manner the real space Green's functions for an isolated inhomogeneity with the help of finite matrices, which makes it relatively adaptable to extend to dense distributions of linear defects in surfaces and interfaces.

References

1. R. Landauer, J. Phys. Cond. Matter **1**, 899 (1989).
2. B. Shapiro, Phys. Rev. Lett. **65**, 1510 (1990).
3. S. de Gironcoli, S. Baroni, Phys. Rev. Lett. **63**, 1959 (1992).
4. Y. Meir, S. Wingreen, Phys. Rev. Lett. **68**, 2512 (1992).
5. A. Tekman, P.F. Bagwell, Phys. Rev. B **48**, 2553 (1993).
6. C. Berthod, F. Gagel, K. Maschke, Phys. Rev. B **50**, 18299 (1994).
7. A. Fellay, F. Gagel, K. Maschke, A. Virlouvet, A. Khater, Phys. Rev. B **55**, 1707 (1997).
8. A. Virlouvet, A. Khater, K. Maschke, H. Aouchiche, O. Rafil, Phys. Rev. B **59**, 4933 (1999).
9. A. Khater, J. Szeftel, Phys. Rev. B **35**, 6749 (1987); D.O. Edwards, R.C. Pandorf, Phys. Rev. A **140**, 816 (1965).
10. I. Lyuksyutov, A.G. Naumovets, V. Pokrovsky, *Two-Dimensional Crystals* (Academic Press, 1992).
11. M.A. Chesters, M. Hussain, J. Pritchard, Surf. Sci. **35**, 161 (1973).
12. K. Kern, R. David, P. Zeppenfeld, G. Comsa, Surf. Sci. **195**, 353 (1998).
13. A.D. Novaco, J.P. McTague, Phys. Rev. Lett. **38**, 1286 (1977).
14. M. Kardar, A.N. Berker, Phys. Rev. Lett. **48**, 1552 (1982).
15. A. Glebov, J.R. Manson, S. Miret-Artes, J.G. Skofronick, J.P. Toennies, Phys. Rev. B **57**, 9455 (1998); A.P. Graham, M.F. Bertino, F. Hoffmann, J.P. Toennies, Ch. Wöll, J. Chem. Phys. **106**, 6194 (1997).
16. A. Maradudin, R.F. Wallis, L. Dobrzynski, *Handbook of Surfaces and Interfaces* (Garland, New York, 1980), Vol. 3.
17. P. Hecquet, B. Salanon, Surf. Sci. **366**, 415 (1996).
18. Y. Pennec, A. Khater, Surf. Sci. Lett. **348**, 82 (1995); A. Virlouvet, H. Grimech, A. Khater, Y. Pennec, K. Maschke, J. Phys. Cond. Matter **8**, 7589 (1996).